

## Laboratory characterisation of the fatigue behaviour of a glass fibre grid-reinforced asphalt concrete using 4PB tests

Ioana Maria Arsenie, Cyrille Chazallon, Jean-Louis Duchez & Pierre Hornych

**To cite this article:** Ioana Maria Arsenie, Cyrille Chazallon, Jean-Louis Duchez & Pierre Hornych (2016): Laboratory characterisation of the fatigue behaviour of a glass fibre grid-reinforced asphalt concrete using 4PB tests, Road Materials and Pavement Design, DOI: [10.1080/14680629.2016.1163280](https://doi.org/10.1080/14680629.2016.1163280)

**To link to this article:** <http://dx.doi.org/10.1080/14680629.2016.1163280>



Published online: 24 Mar 2016.



Submit your article to this journal [↗](#)



View related articles [↗](#)



View Crossmark data [↗](#)

---

## Laboratory characterisation of the fatigue behaviour of a glass fibre grid-reinforced asphalt concrete using 4PB tests

Ioana Maria Arsenie<sup>a</sup>, Cyrille Chazallon<sup>a\*</sup>, Jean-Louis Duchez<sup>b</sup> and Pierre Hornych<sup>c</sup>

<sup>a</sup>Laboratoire des sciences de l'ingénieur, de l'informatique et de l'imagerie, ICUBE (UMR 7357, CNRS), Strasbourg Cedex, France; <sup>b</sup>Epsilon Ingénierie, 69480 Anse, France; <sup>c</sup>IFSTTAR, LAMES, Bouguenais Cedex, France

(Received 27 February 2014; accepted 1 March 2016)

This paper presents a complete experimental study of the fatigue behaviour of a glass-fibre-reinforced asphalt concrete, respecting EN 12697-24:2012, Annex D. The study is based on 38 four point bending tests, performed on 18 non-reinforced asphalt specimens and 20 geogrid-reinforced asphalt specimens. Both non-reinforced and reinforced asphalt specimens are tri-layered beams. The reinforced specimens contain two glass fibre grids, each one placed at the interface between two asphalt concrete layers. The objectives of the study were: (1) to characterise the fatigue behaviour of reinforced asphalt concrete, and to determine fatigue parameters, which can be used for pavement design, following the French pavement design method, (2) to show that glass fibre grid delays fatigue crack propagation and (3) to estimate the gain in fatigue due to the geogrid. The comparison of the fatigue curves of non-reinforced and reinforced asphalt concrete indicates that the geogrid increases fatigue life for the testing conditions, which were: fully reverse loading, displacement control, sinusoidal waveform,  $T = 10^{\circ}\text{C}$  and  $f = 25\text{ Hz}$ .

**Keywords:** asphalt concrete; glass fibre grid; fatigue; four point bending test; fully reverse fatigue tests

### 1. Introduction

Since the late 1960s, coated glass fibre grids also known as “geogrids” are used as reinforcement materials in different pavement structures subjected to fatigue cracking. Fatigue cracking is generated by cyclic loadings induced by traffic, temperature gradients and can affect the road base, or only the surface layers. Water infiltrations aggravate fatigue cracking propagation. If it is not prevented, fatigue cracking generates pavement deterioration.

Geogrids are generally used for the rehabilitation of cracked pavements (semi-rigid pavements, asphalt pavements and flexible pavements), but nowadays they are also included in new pavements. Their reinforcement role consists in delaying fatigue crack propagation. For rehabilitation of cracked pavements, geogrids are frequently located in the lower part of the new bituminous overlay, to prevent propagation of cracks from the old pavement and to improve overall fatigue resistance (if the lower layers have a low stiffness, significant tensile stresses can develop in the overlay; Nguyen, Blanc, Kerzreho, & Hornych, 2013). In the French design method for pavement rehabilitation, if the old pavement presents severe deterioration, the tensile

\*Corresponding author. Email: [cyrille.chazallon@insa-strasbourg.fr](mailto:cyrille.chazallon@insa-strasbourg.fr)

stress is calculated at the bottom of the new layers, and the fatigue design criterion is applied only to these new layers.

Most geogrids are installed over a tack coat of bitumen emulsion, which is laid on the top of the old base course, after the milling of the wearing course, or on a new levelling course, which must be flat, smooth, clean and dry, and the cracks must be treated prior to the laying of the geogrid. The tack coat guarantees the bonding of the geogrid with the asphalt layer and the quality of the interface between these two materials. The surface of the grid is usually rolled with a rubber-coated or pneumatic tired roller to improve bonding with the base course.

Relevant in-situ studies carried out in France at IFFSTAR (Kerzreho & Hornych, 2010–2011) and in Italy (Pasquini, Bocci, Ferotti, & Canestrari, 2013) showed that the glass fibre grids delay fatigue crack propagation. Laboratory studies (Agostinacchio & Fiori, 2007; Bacchi, 2009; Ferroti, Canestrari, Virgili, & Grilli, 2011; Pasquini et al., 2013; Virgili, Canestrari, Grilli, & Santagata, 2009) based on four point bending (4PB) and three point bending (3PB) fatigue tests performed with haversine waveform showed that fatigue life of reinforced specimens increases significantly, in different testing conditions. However, in most cases, the cyclic loading applied in these tests is a purely compressive loading, which adds a creep component to the strain response of the specimen, due to the viscoelastic behaviour of bituminous materials. The fatigue 4PB tests in load control with sinusoidal waveform performed on geogrid-reinforced asphalt slabs by Brown, Thom, and Sanders (2000) showed that the geogrid reduces the rate of crack propagation in the asphalt layers situated below and above it.

The objective of this study was to try to determine, for grid-reinforced asphalt (GRA) materials, fatigue parameters which can be used in current pavement design methods, based on a fatigue design criterion for asphalt layers. This is in particular the design approach used in the French pavement design method (standard NF P98-086, 2011). This method is based on the following principles:

- A multi-layer linear elastic model is used to calculate the stresses and strains in the pavement under a reference axle load.
- For bituminous layers, the design criterion used is a fatigue criterion, based on the maximum tensile strain  $\varepsilon_t$  at the bottom of the bituminous layers.
- The maximum tensile strain  $\varepsilon_t$  must not exceed a limit fatigue strain, depending on the number of standard axle loads NE, expressed by

$$\varepsilon_t \leq \varepsilon_6(10^\circ\text{C}, 25\text{ Hz}) \cdot \sqrt{\frac{E(10^\circ\text{C}, 10\text{ Hz})}{E(\theta_{\text{eq}}, 10\text{ Hz})}} \cdot [\text{NE}/10^6]^b \cdot k_r \cdot k_s \cdot k_c, \quad (1)$$

with  $\varepsilon_6$  being the strain leading to a fatigue failure for  $10^6$  cycles,  $\theta_{\text{eq}}$  a temperature;  $b$ , the slope of the fatigue line; NE, the number of standard axle loads (130 kN dual wheel axle loads);  $k_r$ ,  $k_s$  and  $k_c$  are coefficients related respectively with the risk of failure, the bearing capacity of the soil and the calibration of the model.

The French pavement design approach based on fatigue behaviour has been evaluated by comparison with field data, and accelerated full scale tests, and this has led to the determination of calibration factors, relating laboratory and field behaviour. Details about the method and the calibrations can be found in Corte and Goux (1996) and Odéon, Gramsammer, and Caroff (1997).

The fatigue approach described above supposes that the tested material is homogeneous, and the applicability of this assumption for grid-reinforced layers will be discussed later.

To characterise experimentally the fatigue behaviour of a glass fibre GRA concrete, a specific fatigue test was developed. To evaluate the reinforcement benefit, the results were compared to

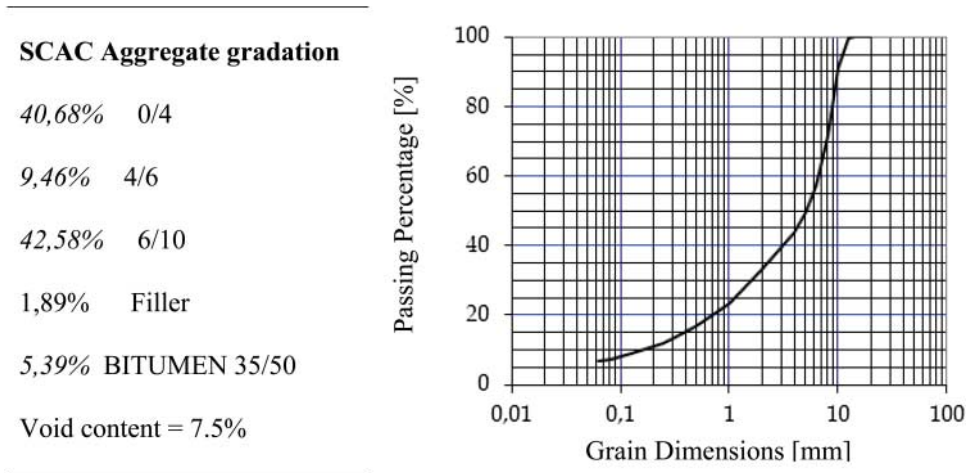


Figure 1. Aggregate gradation and grading curve of SCAC 0/10 class III.

the same non-reinforced asphalt (NRA) concrete, characterised following the European fatigue standards (EN 12697-24, 2012). Consequently, the same test procedure was used for these two studies in order to show that the geogrid delays fatigue crack propagation. The characterisation of the fatigue behaviour of the NRA and the GRA was made with fatigue 4PB tests. A large 4PB testing device was designed for the study (Arsenie, 2013), considering the geogrid dimensions and the European fatigue standards. The beam dimensions chosen are 630 mm in length by 100 mm in width and 100 mm in height.

To obtain a realistic fatigue test, complying with the European standard of the 4PB test (EN 12697-24, 2012), a loading system, using clamps, that allows us to perform alternate tension-compression loading, with strain control, was designed. In order to achieve a symmetrical, alternate loading, it was also decided to use “double reinforced beams”, including two geogrids, placed symmetrically below and above the neutral axis of the beam, at heights of 25 and 75 mm.

This paper is organised as follows. Section 2 presents the tested materials and their characteristics, the testing device and the sample preparation. Section 3 presents the 4PB testing procedure, the experimental programme, the results and their analysis. Section 4 provides the conclusions of the study.

## 2. Materials and testing device

### 2.1. Asphalt concrete

The tested asphalt concrete is a classic formula of SCAC (semi-coarse asphalt concrete) 0/10 mm class III, according to the European classification (EN 13108-1, 2007), currently used for wearing courses. The aggregates (granite, amphibole and leptynite) have a maximum size of 10 mm and come from Courzieu quarry in France. The binder is a bitumen class 35/50, according to the European Classification (EN 12591, 2009). The SCAC formula and grading curve are presented in Figure 1. The stiffness modulus  $E$  is 9 GPa and it has been determined in 4PB tests, performed at  $T = 5^{\circ}\text{C}$  with  $f = 10$  Hz (Arsenie, 2013).

### 2.2. Glass fibre grid

The geogrid is a coated fibre glass grid, shown in Figure 2. The product is an elastic composite made of warp yarns, filling yarns and nonwoven parts of polyester fibre, with a mesh

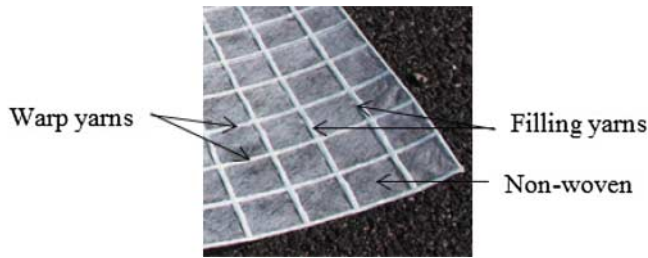


Figure 2. Geogrid. Geometry and composition.

of  $40 \times 40 \text{ mm}^2$ . The warp and filling yarns are made of continuous *E* fibre glass roving and styrene butadiene styrene (SBS) resin. In practice, the geogrid is bonded to the pavement layers by applying a tack coat containing 65% of residual bitumen.

The geogrid tensile strength at failure is 100 kN/m. Its Young modulus is 44 GPa (Themeli, 2011), average value determined from three methods (tensile strength test, loading–unloading tensile tests and mixing law). The endurance limit of the warp and filling yarns was studied with cyclic tensile fatigue displacement controlled tests in Sagnol (2013), where the endurance limit is larger than 2‰.

### 2.3. 4PB device

#### 2.3.1. Choice of the test configuration

The RILEM interlaboratory fatigue tests study (Di Benedetto, De la Roche, Baaj, Pronk, & Lundstrom, 2004) compared the results of five types of tests (tension–compression T/C, two point bending (2PB), 3PB, 4PB and indirect tensile test, ITT) and showed that the fatigue life depends on the type of test (homogeneous or non-homogeneous) and mode of loading. The results from the beam tests (2PB, 3PB and 4PB) seemed to depend on the kind of test and specimen size. However, the 2PB and 4PB beam tests were found to give the most comparable results.

In order to find an appropriate testing configuration for the geogrid-reinforced asphalt concrete, two types of fatigue tests could be considered: 3PB test and 4PB test. The 3PB test configuration adds a shear component to crack propagation, which is not present in the 4PB test configuration, where crack propagation occurs in mode I (between the applied loads). The 4PB test importance is recognised by Huurman and Pronk (2009) and it is preferred because failure is believed to happen in an area of uniform bending moment with no vertical shear stress, corresponding to the central part of the beam, between the two loading lines. Equations of the beam theory can be applied if the hypothesis of an elastic homogeneous isotropic material is considered.

In this work, where the objective was to apply a “standard” fatigue approach, it was considered that the geogrid is perfectly bonded with the asphalt concrete, by use of a tack coat. Neither the shear phenomenon, nor the possible slip of the grid inside the specimen structure was taken into consideration.

#### 2.3.2. 4PB device

The 4PB device (Figure 3) used in this work was designed in order to test asphalt concrete beams reinforced with glass fibre grids, following the European fatigue standard. The device was designed for  $630 \times 100 \times 100 \text{ mm}^3$  asphalt concrete beams. These dimensions resulted from three conditions:



Figure 3. 4PB device (Arsenie, 2013).

- The beam width has been fixed to 100 mm, in order to include a minimum three warp yarns.
- The beam height has been fixed to 100 mm, in order to be able to test beams with two geogrids, placed as far as possible from the neutral axis of the beam, and to perform fatigue test with fully symmetrical, alternate loading.
- The length between the supports of the beam has been chosen equal to six times the height or the width of the beam, according to Annex D of EN 12697-24 (2012). It resulted in a beam length  $L = 630$  mm.

#### 2.4. Sample preparation

Two types of samples were made in the laboratory: NRA and geogrid-reinforced asphalt samples. The preparation of the asphalt concrete slabs was performed in five steps, (Figure 4), as follows:

- Compaction of the first asphalt concrete layer of 50 mm.
- Insertion of the first geogrid with 600 g/m<sup>2</sup> of tack coat (65% of residual bitumen) at room temperature. For NRA beams, a quantity of 400 g/m<sup>2</sup> of tack coat (65% of residual bitumen) was used.
- Compaction of the second asphalt concrete layer of 50 mm.
- Insertion of the second geogrid with 600 g/m<sup>2</sup> of tack coat at room temperature. For NRA beams, a quantity of 400 g/m<sup>2</sup> of tack coat was used.
- Compaction of the third asphalt concrete layer of 50 mm.

The compaction was performed with a rolling wheel compactor BBPAC–LCPC and consisted in a total number of 92 wheel passes, carried out in three different wheel positions (36 passes in the front position – 20 passes in the centre position – 36 passes in the rear position) with a 10 kN load, according to EN 12697-33. A steel cylinder was rolled over the geogrid to improve the bonding.



Figure 4. Insertion and installation of the geogrid on the bitumen emulsion layer.



Figure 5. Three-layered asphalt slab, reinforced with two geogrids.

Three beams of  $630 \times 100 \times 100 \text{ mm}^3$  were sawed from each slab, where the geogrids were symmetrically positioned at  $h = 25$  and  $h = 75$  mm of the beam height (Figure 5). As explained previously, the two grids were necessary to obtain a symmetrical specimen, and their vertical position at 25 and 75 mm was chosen in order to have a sufficient cover of asphalt concrete above the grid. The objective was not to reproduce exactly the position of the grid in the field.

### 3. 4PB tests and results

#### 3.1. Testing procedure

The standard 4PB test was performed under sinusoidal alternating loading conditions. The tests performed in this study were displacement controlled tests (commonly called constant strain). The vertical displacement at the centre of the beam was measured on the bottom side with a linear variable displacement transducer. The force response and the phase angle were measured all along the test (Figure 6).

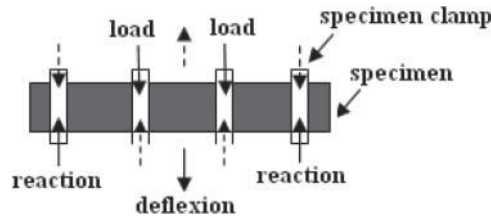


Figure 6. Principle of the alternating 4PB test.

### 3.2. Experimental programme

After preparation, all the specimens have been kept around three weeks in the laboratory at constant temperature  $T = 20^{\circ}\text{C}$ . Before testing, the specimens have been conditioned around 12 h in the conditioning chamber of the testing device, at constant temperature  $T = 10^{\circ}\text{C}$ . This assures a constant temperature throughout the specimen before the test, which is maintained constant all along the test.

The experimental programme consisted of 38 4PB fatigue tests, performed at  $T = 10^{\circ}\text{C}$  and  $f = 25$  Hz, on 18 NRA specimens and 20 GRA specimens. The 18 NRA specimens were tested at 3 strain levels: 6 tests at  $150\ \mu\text{m/m}$ , 6 tests at  $135\ \mu\text{m/m}$ , 6 tests in the range  $(111; 116)\ \mu\text{m/m}$ . The 20 GRA specimens were tested at 4 strain levels: 6 tests at  $150\ \mu\text{m/m}$ , 6 tests at  $135\ \mu\text{m/m}$ , 6 tests in the strain range  $(126; 129)\ \mu\text{m/m}$  and 2 tests at  $115\ \mu\text{m/m}$ . This approach is based on the principle of the standard of the fatigue test (EN 12697-24, 2012), which requires to make fatigue tests at three strain levels, with a minimum of six tests per stress level. In addition, the strain levels must be chosen in order to have fatigue lives in the range:  $10^4$  to  $2 \times 10^6$  cycles.

### 3.3. Results

First we have to mention that no delamination of the beams, observed visually, occurs during all the tests. The loss of stiffness was only due to bottom-up and top-down crack propagations between the loading lines. For the interpretation of the test results, the composite material is considered as a homogenous material, which fatigue characteristics have been improved. This point is discussed in Section 3.4.1.

Fatigue tests results are presented in Table 1, using the fatigue life  $N_f$  defined in European fatigue standards (EN 12697-24, 2012) as the number of loading cycles  $N$  giving a loss of 50% of the initial dynamic modulus  $E_i$ .

Figures 7 and 8 present the fatigue damage  $(E/E_i - N)$  curves for the NRA and GRA specimens. Three  $(E/E_i - N)$  curves are represented for each strain level: the fatigue damage curves giving the minimum and maximum fatigue lives, and the average fatigue damage curve.

### 3.4. Result analysis

#### 3.4.1. Classical analysis

To analyse the fatigue 4PB tests, the following assumptions have been made:

- The composite material was considered as a homogenous material, which fatigue characteristics have been improved. The vertical position of the grid was chosen in order to have a sufficient cover of asphalt concrete above the grid and a composite material more representative of the in situ behaviour of the reinforced layer. It was not possible to have



Table 1. Fatigue test results with NRA and GRA specimens.

Specimens NRA		Specimens GRA	
Deformation $\varepsilon$ [ $\mu\text{m}/\text{m}$ ]: 150		Deformation $\varepsilon$ [ $\mu\text{m}/\text{m}$ ]: 150	
Average $N_{f,NRA}$ [cycles]	257 873	Average $N_{f,GRA}$ [cycles]	354 240
Fatigue line ( $\log_{10}(N_f)_{NRA}$ )	242 917	Fatigue line ( $\log_{10}(N_f)_{GRA}$ )	374 532
Deformation $\varepsilon$ [ $\mu\text{m}/\text{m}$ ]: 135		Deformation $\varepsilon$ [ $\mu\text{m}/\text{m}$ ]: 135	
Average $N_{f,NRA}$	414 752	Average $N_{f,GRA}$	724 416
Fatigue line ( $\log_{10}(N_f)_{NRA}$ )	423 965	Fatigue line ( $\log_{10}(N_f)_{GRA}$ )	695 089
Deformation $\varepsilon$ [ $\mu\text{m}/\text{m}$ ]: 111–116		Deformation $\varepsilon$ [ $\mu\text{m}/\text{m}$ ]: 126–129	
Average $N_{f,NRA}$	1,097,290	Average $N_{f,GRA}$	1,095,474
Fatigue line ( $\log_{10}(N_f)_{NRA}$ )	1,070,349	Fatigue line ( $\log_{10}(N_f)_{GRA}$ )	983,059
		Deformation $\varepsilon$ [ $\mu\text{m}/\text{m}$ ]: 115	
		Average $N_{f,GRA}$	1,435,665
		Fatigue line ( $\log_{10}(N_f)_{GRA}$ )	1,807,774

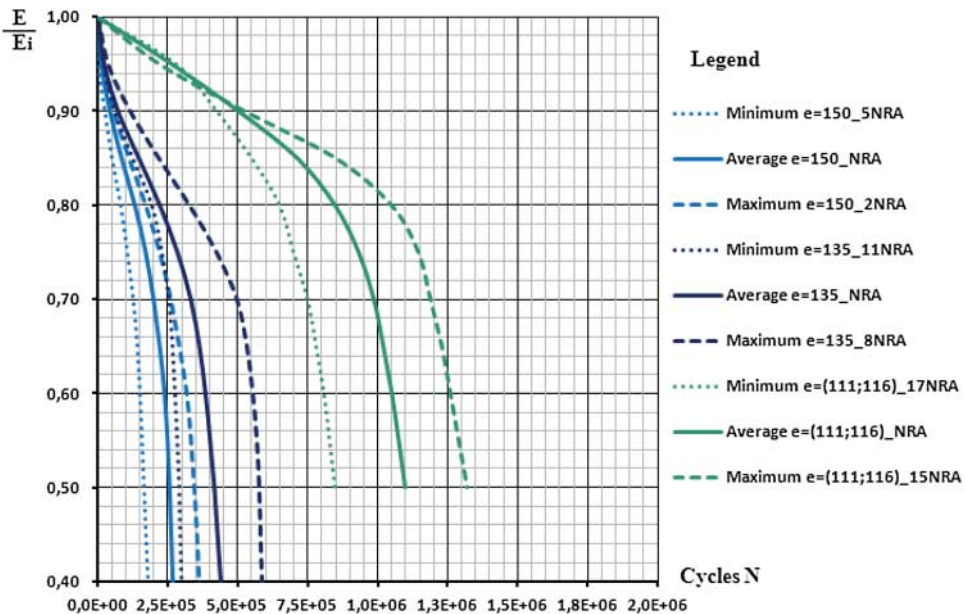


Figure 7. Fatigue damage curves of NRA specimens corresponding to maximum and minimum fatigue life, average fatigue damage at  $\varepsilon = 150; 135; 116; 111 \mu\text{m}/\text{m}$ .

a thinner asphalt concrete layer at the bottom and the top of the beam, for producing high-quality specimens (to ensure good bonding and compaction). The solution to glue grids on the top and bottom faces of the beam was not considered realistic. The glass fibre grid volume in the GRA specimens was considered negligible, representing 0.456% of the volume of the specimen.

- The hypothesis of a perfect bonding between the geogrids and asphalt concrete layers. This is supported by the tack coat applied with the geogrid, which provided good bonding with the subsequent asphalt layer, placed over the geogrid and compacted.
- The fatigue induced by shear stresses is minimised in the 4PB test configuration.

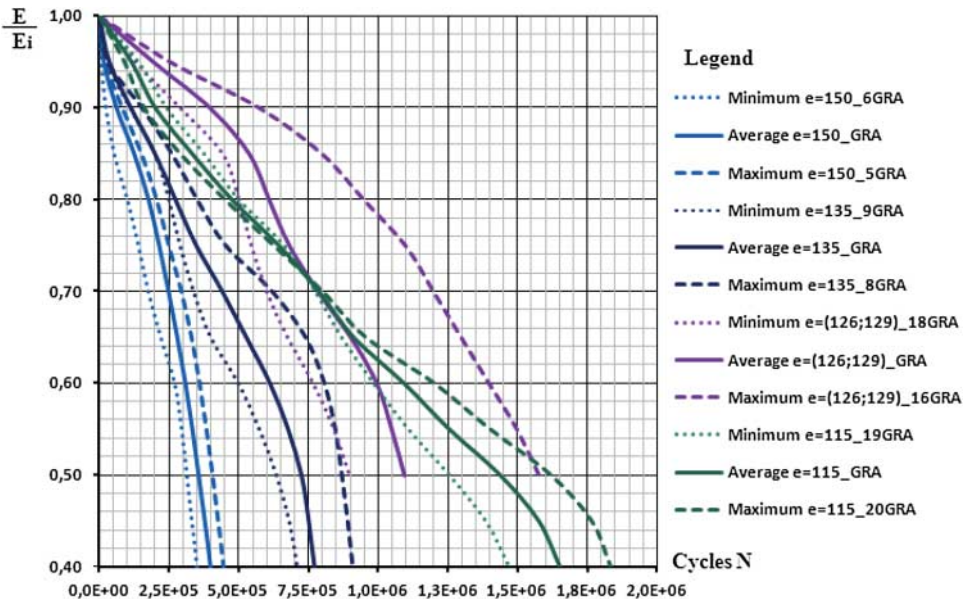


Figure 8. Fatigue curves of GRA specimens corresponding to maximum and minimum fatigue life, average fatigue damage at  $\varepsilon = 150; 135; 129; 126; 115 \mu\text{m/m}$ .

With these assumptions, it was possible to use the classical analysis of the fatigue tests with Wohler curves. The results presented in Table 1 were used to calculate the fatigue curves (Figure 8) of the NRA concrete (2) and geogrid-reinforced asphalt concrete (3), according to EN 12697-24 (2012).

$$\log_{10} N_f = -14.853 - 5.293 \log_{10} \varepsilon, \quad (2)$$

$$\log_{10} N_f = -17.000 - 5.904 \log_{10} \varepsilon. \quad (3)$$

The tensile strain  $\varepsilon_6$ , leading to a fatigue life  $N_f = 10^6$  cycles, was calculated from Equations (2) and (3), respectively:  $\varepsilon_6 = 115 \mu\text{m/m}$  for NRA and  $\varepsilon_6 = 127 \mu\text{m/m}$  for GRA. These values are high, typical values of  $\varepsilon_6$  for French pavement materials are in the range 90–120  $\mu\text{m/m}$  (for a SCAC the reference value in the French design method is  $\varepsilon_6 = 100 \mu\text{m/m}$ ). From the comparison of  $\varepsilon_6$  values, it results that the glass fibre grid increases  $\varepsilon_6$  by 10.52%. The comparison of Equations (2) and (3) shows that the glass fibre grid also increases the fatigue curve slope by 11.55%. These variations are significant, when applying the French pavement design method (NF P98-086, 2011), which is based on the comparison of the tensile strain calculated at the bottom of the asphalt layer with the maximum design tensile strain, defined by Equation (1). The maximum design strain is a function of traffic, the tensile strain  $\varepsilon_6$  and the fatigue curve slope, determined from standardised laboratory fatigue tests (Figure 9).

The  $(E/E_i - N)$  curves (Figures 7 and 8) for each strain level characterise the evolution of the average fatigue life, which increases with the decrease of the strain level. In Figure 8, there is an intersection between the  $(E/E_i - N)$  curves at  $\varepsilon = (126; 129) \mu\text{m/m}$  and  $\varepsilon = 115 \mu\text{m/m}$ , which can probably be explained by experimental scatter due to the small number of 4PB tests at  $\varepsilon = 115 \mu\text{m/m}$  (two tests only). However, the average fatigue life at  $\varepsilon = 115 \mu\text{m/m}$  is higher than the one at  $\varepsilon = (126; 129) \mu\text{m/m}$ .

The gain due to the geogrid was calculated for each strain level, as the ratio between the average fatigue lives of the reinforced and NRA concrete specimens  $N_{f, \text{GRA}}/N_{f, \text{NRA}}$ . The ratio is

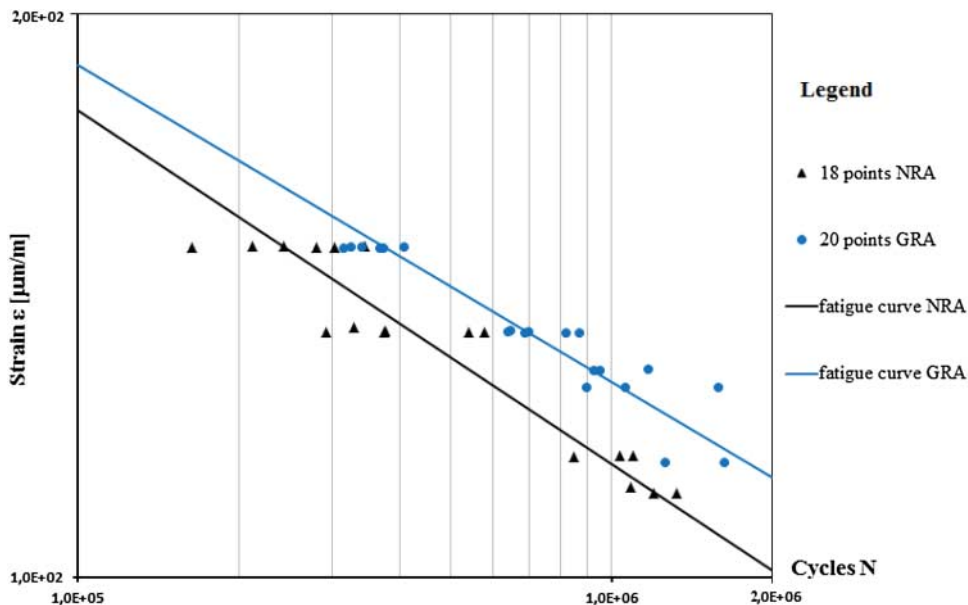


Figure 9. Experimental points NRA and GRA and fatigue curves NRA and GRA.

Table 2. Fatigue life ratios  $N_{f,GRA}/N_{f,NRA}$  from experimental results and fatigue lines.

Strain $\epsilon$ [ $\mu\text{m}/\text{m}$ ]	Experimental results			Fatigue lines		
	$N_{f,GRA}$	$N_{f,NRA}$	$N_{f,GRA}/N_{f,NRA}$	$N_{f,GRA}$	$N_{f,NRA}$	$N_{f,GRA}/N_{f,NRA}$
150	354,240	257,873	1.37	374,532	242,917	1.54
	Six tests	Six tests		Eq. (3)	Eq. (2)	
135	724,416	414,752	1.75	695,089	423,965	1.63
	Six tests	Six tests		Eq. (3)	Eq. (2)	
115	1,435,665	1,034,805	1.39	1,807,774	1,070,349	1.68
	Two tests	Six tests		Eq. (3)	Eq. (2)	
	Average $N_{f,GRA}/N_{f,NRA}$		1.50	Average $N_{f,GRA}/N_{f,NRA}$		1.62

calculated at three strain levels (150, 135 and 115  $\mu\text{m}/\text{m}$ ) in Table 2. The strain level range (126; 129)  $\mu\text{m}/\text{m}$  was not considered, because of the lack of 4PB tests on NRA specimens at these strain levels.

The average ratio  $N_{f,GRA}/N_{f,NRA}$  calculated from the individual test results for the three selected strain levels is 1.50, which means that the geogrid increases by 50% the fatigue life of the NRA concrete. The ratio  $N_{f,GRA}/N_{f,NRA}$  calculated from the fatigue curves is 1.62, meaning that the geogrid increases by 62% the fatigue life of the NRA concrete. These values are close to each other and show that the geogrid delays fatigue crack propagation and behaves as a reinforcement in the asphalt concrete under fatigue loading.

### 3.4.2. Statistical analysis

The French pavement design guide (NF P98-086, 2011) considers that experimental fatigue test results expressed as the logarithm of the fatigue life  $\log_{10}(N_f)$  follow a normal distribution with a standard deviation  $S$ . The standard deviation  $S$  (4) is taken into consideration in a probabilistic

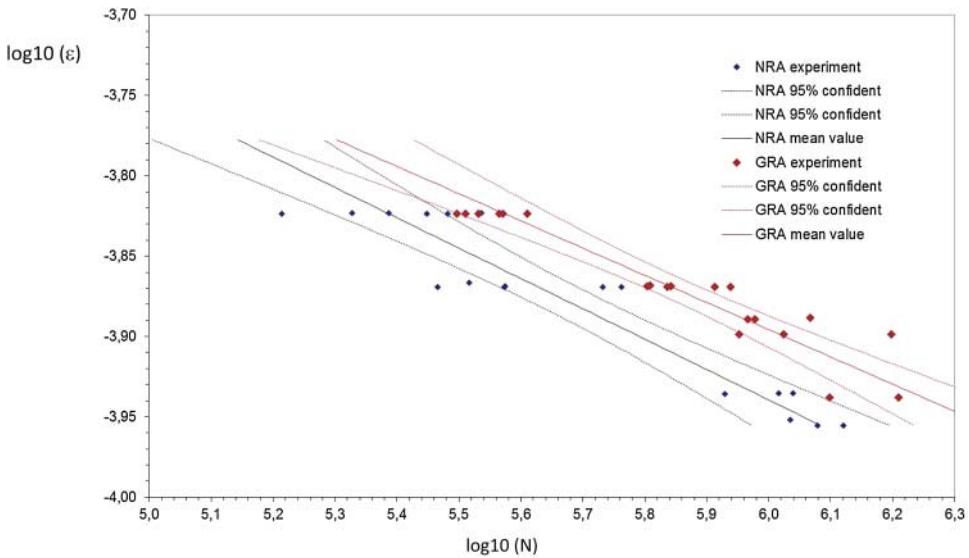


Figure 10. Fatigue lines of NRA and GRA, with confidence intervals at 95%.

Table 3. Strains  $\epsilon_6$  for a fatigue life  $N_f = 10^6$  cycles and their confidence intervals at 95%.

	Minimum value	Mean value	Maximum value
NRA	$\epsilon_{6\_min} = 109 \mu\text{m/m}$	$\epsilon_6 = 115 \mu\text{m/m}$	$\epsilon_{6\_max} = 119 \mu\text{m/m}$
GRA	$\epsilon_{6\_min} = 124 \mu\text{m/m}$	$\epsilon_6 = 127 \mu\text{m/m}$	$\epsilon_{6\_max} = 130 \mu\text{m/m}$

pavements design approach. This statistical analysis of the fatigue tests results using the fatigue curves NRA and GRA was made in order to show that the 4PB tests results follow normal distributions.

$$S = \sqrt{\frac{\sum_{j=1}^l \sum_{i=1}^n [\log_{10}(N_{f,ij}) - \log_{10}(N_{f,j})]^2}{N}}, \tag{4}$$

where  $N_{f,ij}$  is the experimental fatigue life of the specimen,  $i$  at the strain level,  $j$ ;  $N_{f,j}$  is the fatigue life at the strain level,  $j$ , calculated from the fatigue curve;  $i$  is the index of the specimen;  $n$  is the number of specimens;  $j$  is the strain level;  $l$  is the number of strain levels and  $N$  is number of fatigue tests.

The fatigue curves NRA and GRA were represented in the axis system  $\log_{10}(N)/\log_{10}(\epsilon)$  and translated vertically with the corresponding standard deviation  $\pm S$ . Figure 10 represents the fatigue curves of NRA and GRA with their confidence intervals at 95%. The confidence intervals at 95% for the parameter  $\epsilon_6$  are given in Table 3. The results confirm that statistically, the difference between the fatigue curves of the NRA and GRA is significant, and that the experimental scatter is less important with the grid.

#### 4. Conclusions

The objective of this experimental work was to characterise the fatigue behaviour of a geogrid-reinforced asphalt concrete (GRA), composed of a SCAC 0/10 mm and a coated glass fibre grid.

This behaviour was compared with the fatigue behaviour of the NRA concrete, determined using standard European fatigue tests (standard EN 12697-24, Annex D, 2012). This allowed us to demonstrate the role of the glass fibre grid in the asphalt concrete beams submitted to alternate 4PB fatigue tests, in accordance with a standard fatigue test approach.

The fatigue tests were performed with a large size 4PB testing equipment, specially developed for this study. The fatigue curve of GRA was calculated from 20 4PB fatigue tests, performed on tri-layered asphalt concrete beams, where two geogrids were symmetrically positioned at 25 and 75 mm in the beam height. In addition, 18 4PB fatigue tests were performed on tri-layered NRA concrete beams, which permitted to calculate the fatigue curve of the NRA. The dimensions of all the specimens were  $630 \times 100 \times 100 \text{ mm}^3$ .

The comparison of the fatigue curves of GRA and NRA showed the roles of the geogrid in the asphalt structure:

- Increase of the fatigue life  $N_f$  by 50% (based on individual tests) to 62% (based on fatigue curves).
- Increase of the tensile strain  $\varepsilon_6$  by 10.52%.
- Increase of the fatigue curve slope by 11.55%.

The increased tensile strain  $\varepsilon_6$  and fatigue curve slope are relevant for the French pavement design method, to calculate the allowable tensile strain for design, at the bottom of the glass fibre GRA concrete layer.

The evolution curves of the stiffness ratio  $E/E_i$  with the number of cycles  $N$  were represented at different strain levels: 150, 135, (126; 129), (111; 116) and 115  $\mu\text{m/m}$ . The comparison of the fatigue damage curves ( $E/E_i - N$ ) of GRA and NRA specimens showed that the geogrid delays fatigue crack propagation and consequently increases the fatigue life of the asphalt concrete.

A statistical analysis of the 4PB fatigue tests results of both non-reinforced and geogrid-reinforced asphalt concrete was made using the fatigue curves GRA and NRA. This permitted us to show that the fatigue test results on NRA and GRA specimens follow normal distributions, as assumed in the French pavement design standard (NF P98-086, 2011).

These results, showing the increase of the fatigue life of fibre glass GRA concrete, have been obtained for one set of test conditions (temperature 10°C, frequency 25 Hz, fixed position of the grids, placed at 25 mm from the neutral axis of the beam). To generalise these results, it appears necessary, in particular, to take into account the effects of two important parameters:

- The temperature (which will modify the stiffness of the asphalt layer, and thus the relative ratio between the stiffness of the asphalt layer and of the grid),
- The vertical position of the grid, which, in practice, depends on the chosen pavement structure. A possible approach could be to describe the reinforcement (grid + surrounding asphalt material) as a thin, homogeneous layer, with “equivalent” mechanical properties (modulus, fatigue parameters  $\varepsilon_6$  and  $b$ ), integrated in the multilayer pavement structure.

Further studies will be carried out to evaluate the effect of these parameters. Then, it is also planned to make comparisons with full-scale pavement tests, to validate and calibrate the proposed fatigue law, in view of application to pavement design. Such calibration is necessary to take into account the differences between laboratory and field condition, due to such effects as differences in stress states and loading frequency, healing and size effects.

## Disclosure statement

No potential conflict of interest was reported by the authors.

## References

- Agostinacchio, M., & Fiori, F. (2007). *A finite element model to evaluate the role of interlayer fiberglass geogrids in retarding reflective cracking in flexible pavements*. Paper presented at international conference on advanced characterisation of pavement and soil engineering materials. Taylor and Francis Group, London.
- Arsenie, I. (2013, November 29). *Study and modelling of the pavement reinforcement with glass fibre grids under fatigue loading* (PhD thesis). INSA de Strasbourg (National Institute of Applied Sciences), Strasbourg.
- Bacchi, M. (2009). Analysis of the variation in fatigue life through four-point bending test. In Pais (Ed.), *Proceedings of the 2nd workshop on four point bending* (pp. 205–215). Guimaraes, Portugal: University of Minho.
- Di Benedetto, H., De la Roche, C., Baaj, H., Pronk, A., & Lundstrom, R. (2004). Fatigue of bituminous mixtures. Rilem TC182-PEB performance testing and evaluation of bituminous materials. *Materials and Structures*, 37, 202–216.
- Brown, S. F., Thom, N. H., Sanders, P. J. (2000). *Reinforced asphalt* (Final report. No. PGR 99 025). University of Nottingham, p. 25.
- Corte, J. F., & Goux, M. T. (1996). Design of pavement structures: The French technical guide. *Transport Research Report*, 1539, 116–124.
- EN 12591. (2009, December). Spécifications des bitumes routiers. Bitumes et liants bitumineux.
- EN 12697-24. (2012, August). Méthodes d'essai pour mélange hydrocarboné à chaud, Partie 24: Résistance à la fatigue.
- EN 13108-1. (2007, February). Spécifications des matériaux. Partie1: Enrobés bitumineux.
- Ferroti, G., Canestrari, F., Virgili, A., & Grilli, A. (2011). A strategic laboratory approach for the performance investigation of geogrids. *Construction and Building Materials*, 25(2011), 2343–2348.
- Huurman, P., & Pronk, A. C. (2009). Theoretical analysis of the 4point bending test. In A. Loizos, M. N. Partl, T. Scarpas, & L. Al-Quadi (Eds.), *Advanced testing and characterization of bituminous materials* (pp. 3–12). London: Taylor and Francis Group.
- Kerzreho, J. P., & Hornych, P. (2010–2011). Enrobé armé de grille en fibre de verre. *Revue générale des routes et de l'aménagement*, N° 890.
- NF P98-086. (2011, October). Dimensionnement structurel des chaussées routières - Application aux chaussées neuves.
- Nguyen, M. L., Blanc, J., Kerzreho, J. P., & Hornych, P. (2013). Review of glass fibre grid use for pavement reinforcement and APT experiments at IFSTTAR. *Road Materials and Pavement Design*, 14, 287–308. doi:10.1080/14680629.2013.774763
- Odéon, H., Gramsammer, J. C., & Caroff, G. (1997). *Asphalt mix fatigue behavior: Experimental structures and modeling*. Paper presented at the proceedings of the 8th international conference on asphalt pavements, Seattle (USA), August 10–14, pp. 881–897.
- Pasquini, E., Bocci, M., Ferotti, G., & Canestrari, F. (2013). Laboratory characterization and field validation of geo-grid reinforced asphalt pavements. *Road Materials and Pavement Design*, 14(1), 17–35. doi:10.1080/14680629.2012.735797
- Sagnol, L. (2013). *Etude de la grille en fibre de verre pour le renforcement de l'infrastructure* (Master thesis). INSA de Strasbourg and University of Karlsruhe.
- Themeli, A. (2011). *Etude de la fatigue de bétons bitumineux renforcés par des grilles en fibre de verre* (Master thesis). The Institute National Polytechnique of Lorraine and INSA de Strasbourg, Strasbourg.
- Virgili, A., Canestrari, F., Grilli, A., & Santagata, F. A. (2009). Repeated load test on bituminous systems reinforced by geosynthetics. *Geotextils and Geomembranes*, 27, 187–195.